Potential of *Hibiscus sabdariffa* linn. in managing *Fgf21* resistance in diet-induced-obesity rats via *miR-34a* regulation

Neng Tine Kartinah
Universitas Indonesia Fakultas Kedokteran
Nisa Komara
Universitas Indonesia Fakultas Kedokteran
Nuraini Diah Noviati
Universitas Indonesia Fakultas Kedokteran
Syarifah Dewi
Universitas Indonesia Fakultas Kedokteran
Sophie Yolanda
Universitas Indonesia Fakultas Kedokteran
Afifa Radhina
Universitas Indonesia Fakultas Kedokteran
Heriyanto Heriyanto
Universitas Indonesia Fakultas Kedokteran
Imelda Rosalyn Sianipar (imelda.rosalyn@ui.ac.id)
Faculty of Medicine, Universitas Indonesia https://orcid.org/0000-0002-1438-096X

Research

Keywords: Obesity, thermogenesis, flavonoids, antiobesity

Posted Date: November 24th, 2020

DOI: https://doi.org/10.21203/rs.3.rs-112182/v1

Version of Record: A version of this preprint was published at Veterinary Medicine and Science on October 23rd, 2021. See the published version at https://doi.org/10.1002/vms3.653.

Abstract

Background

Obesity is a cause of Fgf21 resistance, which affects the browning and thermogenesis process of the adipose tissue. Decreased receptor expression is influenced by microRNA 34a (miR-34a), whose expression is increased in obesity. While Fgf21-based therapies have been widely investigated, the potential activity of Hibiscus sabdariffa Linn extract (HSE) against Fgf21 resistance is unknown. This study aims to determine the effects of HSE on the expression of miR-34a and Fgf21 receptors in white adipose tissue.

Methods

This experimental study used 24 male Sprague-Dawley rats and divided into four groups: Control (N); diet-induced-obesity rats (DIO); DIO rats with HSE 200 mg/kgBW/day and DIO rats with HSE 400 mg/kgBW/day. Rats were fed a high-fat diet for 17 weeks. HSE was administered daily for five weeks. The administration of HSE 400 mg/kg BW/day resulted in the equivalent expression of miR-34a to that of the control ($p > 0.05$).

Results

Fgfr1 receptor expression was also similar to controls ($p > 0.05$). Beta-klotho expression was significantly lower than that of Control ($p < 0.05$) but equivalent to that of DIO rats ($p < 0.05$).

Conclusions

H. sabdariffa has the potential to reduce Fgf21 resistance in DIO rats through the suppression of miR-34a expression and an increase in the number of Fgfr1 and beta-klotho receptors in adipose tissue.

1. Background

Obesity causes low-grade systemic inflammation, which has an impact on tissue disruption. Systemic low-grade inflammation is caused by an increase in proinflammatory cytokines due to hypoxia of the adipose tissue. Cell hypertrophy causes hypoxia of the adipose tissue, resulting in macrophage infiltration and changing the phenotype of anti-inflammatory macrophages (M2) to proinflammatory macrophages (M1)[1]. One of the effects of chronic inflammation is the increased expression of microRNAs that induces the silencing of the target gene[2]. Proinflammatory cytokines, such as tumor necrosis factor alpha (TNFα) and interleukin 6 (IL-6), increase the expression of microRNAs like miR-34a. In obesity, the expression of miR-34a increase function as a regulator of fibroblast growth factor receptor

1 (Fgfr1) receptor expression and beta-klotho co-receptor that binds to fibroblast growth factor 21 (Fgf21). According to Fu (2016), miR-34a disturbs the Fgf21 signaling cascade in the white adipose tissue through downregulation of Fgfr receptor expression and beta-klotho co-receptor. Disruption of Fgf21 signaling cascade results in Fgf21 resistance in the white adipose tissue[3].

FGF21, a member of the fibroblast growth factor (Fgf) family, located on chromosome 19, is expressed by several organs, including the liver. FGF21 plays a role in controlling the energy homeostasis through the regulation of adipose tissue browning and thermogenesis. Fgf21 must bind to its receptors in the adipose tissue, namely Fgfr1 and beta-klotho, to perform this function. The binding of Fgf21 to its receptors in the adipose tissue activates the Ras/Raf MAPK signaling pathway. Fgf21 induces adipose tissue browning through the increased expression of UCP-1, which plays a role in thermogenic activity, which further increases thermogenesis. Fgf21 binding to its receptor initiates the signal transduction that increases the activity of Sirtuin-1 (SIRT1), then stimulates PGC1α to increase the expression of UCP-1 [3–5].

Considering the potential of FGF21 in browning and thermogenesis, efforts are underway to address work-based obesity through FGF21. Kartinah et al. (2018) found that high-intensity intermittent physical exercise can increase the amount of FGF21 released from the muscle, thereby increasing its activity in the adipose tissue[6]. Sonoda et al. (2017) reviewed many in vivo experiments and showed FGF21 analogs and FGFR agonists that resemble the FGF21 receptor-ligand complex [7]. However, it is still necessary to manage obesity using natural ingredients. Natural ingredients that have the potential to handle obesity include *Hibiscus sabdariffa Linn.* (*H. sabdariffa*), otherwise known as roselle [8, 9].

H. sabdariffa (HSE) contains flavonoids, quercetin, polyphenols, catechins, and anthocyanins [8–10]. The polyphenols in HSE prevent weight gain in diet-induced-obesity [10] rats and inhibit lipogenesis in the white adipose tissue at the molecular level [11].

However, the potential activity of HSE against FGF21 resistance is still unknown. Using an animal model with specific diet to induce obesity and examine the potential activity of HSE against Fgf21 in animal study is necessary before observing its relevance to human biology. This study aims to assess the potential of HSE to act against FGF21 resistance by measuring the expression of its receptors in the adipose tissue (FGFR1 and beta-klotho) and quantifying the levels of the antagonist, miR-34a, in DIO rats.

2. Methods

2.1 Study and Design

The experiments were done in Molecular Biology Laboratory of Faculty of Dentistry, Universitas Indonesia. A sample size of twenty-four rats were counted using Federer's formula. Twenty-four male Sprague-Dawley rats then collected from Animal Facility of Health Research Development, Ministry of Health Republic of Indonesia. The sample (6- 10 weeks age) were randomized into four groups according to extract dosage and metabolic conditions (normal/obesity). The groups were as follows: (1) Control (N);

(2) DIO 12; (3) DIO rats administered with HSE 200 mg/day/kg body weight (BW) (Ob-Hib200); and (4) DIO rats administered with HSE 400 mg/day/kgBW (Ob-Hib400).

Obesity in rats was induced by administering a high-fat diet (19.09% fat, 24.00% protein), while the control group was fed a standard diet. The diets were administered for 17 weeks [13]. Then the rats were included in the obesity list. Rats were categorized as DIO if their Lee index was more than 310. Rats' BW and body length (naso-anal) were measured using the Lee index formula [14] as follows:

$$Lee\ Index = \frac{\sqrt[3]{bodyweight}}{body\ length}\ x\ 1000$$

DIO rats were included in the Ob, Ob-Hib200, or Ob-Hib400 group. *HSE 200 and* 400 mg/day/kgBW doses were based on the research by Andraini and Yolanda (2014) [15]. The high-fat diet was maintained until the end of the study. The Ethical Committee of Faculty of Medicine, Universitas Indonesia approved all experiments, in which 24 male Sprague-Dawley rats (Balitbangkes, Jakarta), 6-10 weeks old, were housed (three rats per cage) following a 12 h:12 h light/dark cycle.

2.2. Provision of *HSE* Methanol Extract

*H. sabdariffa plants*were obtained from the Center for Biopharmaceutical Studies at Bogor Agricultural University. Extraction was performed using maceration with methanol. Dilution of the extract was based on seven days of treatment. After dilution, the preparation was stored at 4°C. Rats that were administered *HSE extract*had to be weighed to determine the amount of extract to be administered. *H. sabdariffa* was administered orally using a gastric sonde once a day for five consecutive weeks for the Ob-Hib 200 and Ob-Hib 400 groups.

2.3 Sampling Technique

Decapitation was performed following anesthesia using a combination of xylazine hydrochloride 0.01 ml/kgBW and 0.05 ml/kgBW ketamine. Rats were left to fast for 12 h before decapitation. Rats were then dissected, and adipose tissue was harvested. The sample was put into a pot and stored in a refrigerator at -80°C. Blood samples from the rats' sinus orbita were collected into EDTA tubes and centrifuged to obtain serum. The serum samples were used for lipid profile measurements, such as total cholesterol and triglyceride levels.

2.4 Measurement of Total Cholesterol and Triglyceride Levels in Rat Serum

Total cholesterol levels were measured using the CHOD-PAP reagent, while triglyceride levels were measured using the GPA-PAP reagent, both for enzymatic colorimetric tests that require the same method. Reagent blank measurement was performed by pipetting 1000 µl R1 into cuvettes and incubating for 5 min. Then, the absorbance of the blank was measured using a spectrophotometer at a wavelength of 500 nm. Standard measurement was performed by pipetting 10 µl of standard and 1000 µl of R1 into cuvettes, which were mixed and incubated for 5 min. Sample measurement was performed by pipetting 10 µl of the sample and 1000 µl of R1 into cuvettes, which were mixed and incubated for 5 min. The absorbance of the standard or sample against the reagent blank (ΔA) was measured at a wavelength of 500 nm. The absorbance results (ΔAstandard and ΔAsample) were then calculated (for mg/dL) as follows:

$$C = 200 \times \frac{\Delta\text{Asample}}{\Delta\text{Astandard}}$$

2.5 Measurement of Fgfr1, beta-klotho Gene (Klb), and miR-34a Expression in the Adipose Tissue

Fgfr1 and *Klb* expression levels were quantified through several stages: 1) RNA isolation using the Quick-RNA MiniPrep Plus (Zymo Research, California, US) kit; 2) synthesis of cDNA (from RNA in stage 1) using the cDNA synthesis kit and a ReverTra Ace® qPCR RT Master Mix with gDNA Remover (Toyobo); 3) real-time PCR was performed in triplicate to measure the expression of *Fgfr1* and *Klb* using the SensiFAST SYBR Hi-ROX Kit (Bioline) kit with a two-step method. RNA concentrations were measured using a nanodrop, and dilutions to obtain the required RNA concentration were performed using nuclease-free water.

Gene expression was then analyzed using the Micro drop VarioSkan Spectrophotometer. Primers used to measure the expression of the Fgfr1 receptor, beta-klotho, and a housekeeping gene are in Table 1. RNA isolation was performed to obtain the RNA necessary for examining *miR-34a* expression. Total RNA isolation from adipose tissue was performed using the Quick-RNA MiniPrep Plus (Zymo Research) kit. cDNA synthesis was performed, such that miRNA could be amplified using real-time PCR. Real-time PCR was performed in triplicate using the miR- 34a Detection and U6 Calibration Kit (Cohesion Biosciences).

2.6 Statistical Analysis

Six samples were used in each analysis. The Shapiro-Wilk normality test was performed on the collected data. If the data were distributed normally, then the analysis was continued using parametric tests with one-way analysis of variance [16]. If the data were not distributed normally and remained abnormal after transformation, a nonparametric test was carried out using the Kruskal-Wallis test. A p-value of <0.05 was considered statistically significant. Paired T-test was used to analyze the lipid profile results and

determine the significance of pre and post HSE treatment. A Sig. (2-tailed) p-value<0.05 was considered statistically significant. Data processing was performed using the SPSS 23 software (Statistical Social Sciences 23).

3. Results

3.1 Effects of H.sabdariffa on Rat Lipid Profile

Our experiments showed that there was no difference between the total cholesterol of pre and post treatment of HSE, as shown in Figure 1. This condition could not explain the influence of HSE treatment, because we were not measuring the low and high density lipoprotein levels.

In pre and post treatment HSE, triglyceride levels were different. After 200mg/KgBW of HSE administration, there was a decrease in triglyceride levels. The treatment groups had lower levels than those of the normal control group. The administration of HSE able to maintain triglyceride levels, such that the value is equivalent to the normal control group (p>0.05).

3.2 Effects of H. sabdariffa on the Lee Index of DIO rats

The Lee index of the Ob group was the highest and was significantly different from that of the control (p<0.001), Ob-Hib200 (p<0.01), and Ob-Hib400 (p<0.001) groups, as shown in Figure 3. In addition, the Lee index of rats administered with *HSE* at doses of 200mg/kgBW and 400mg/kgBW were below 310. The results indicated that the administration of *HSE* reduced the Lee index to normal limits.

3.3 Effects of H. sabdariffa on miR-34a expression in the Rat White Adipose Tissue

There was a higher expression of *miR-34a* in the Ob group compared with that of the N group (p <0.001), as shown in Figure 4. The administration of *HSE* at a dose of 200 mg/kgBW/day could not reduce the expression of *miR-34a* compared with the Ob group (p>0.05), while the administration of extracts at 400 mg/kgBW reduced *miR-34a* expression (p<0.001).

3.4 Effects of H. sabdariffa on Fgfr1 in the Rat White Adipose Tissue

Figure 5 shows *Fgfr1* expression in the rat adipose tissue. *Fgfr1* expression in theOb group was lower compared to that of the N group (p<0.01). The administration of *HSE* in DIO rats at a dose of 400 mg/kgBW maintained the expression of *Fgfr1* at levels equivalent to that of the control group (p>0.05).

Meanwhile the expression of FGFR1 in the DIO rats group administered *HSE* at a dose of 200 mg/kgBW was still low and was significantly different from that of the control rats ($p<0.05$).

3.5 Effects of H. sabdariffa on Klb Expression in Rat White Adipose Tissue

Figure 6 shows *Klb* expression in rat adipose tissue, which indicated that *Klb* expression in the Ob group was lower compared to that of N group ($p<0.001$). However, the administration of *HSE extract* at a dose of 400 mg/kgBW in DIO rats increased the expression of *Klb* significantly compared to that of DIO rats ($p<0.001$) and the DIO rats administered *HSE at a dose of* 200 mg/kgBW ($p<0.01$). However, *Klb* expression in DIO rats treated with *H. sabdariffa at* a dose of 400 mg/kgBW was still lower than that in the control group ($p<0.05$).

3.6 Effects of H. sabdariffa on Ppargc1a expression in Rat White Adipose Tissue

Ppargc1a (encoding PGC1α) expression is shown in Figure 7. We found that *Ppargc1a* expression in DIO rats was lower compared to that of the control group ($p<0.01$). The administration of *HSE* to DIO rats at a dose of 200 mg/kgBW did not increase *Ppargc1a* expression compared to that of the Ob group ($p>0.05$), but a significant difference compared to that of the control group ($p<0.01$) was observed. The administration of 400mg/KgBW HSE to DIO groups increased *Ppargc1a* expression; therefore, the relative expression was not significantly different from that of the control group ($p>0.05$).

3.7 Effects of H. sabdariffa on Ucp-1 expression in Rat White Adipose Tissue

The expression of *Ucp-1* in DIO rats was lower compared to that of the control group, but not significantly different, as shown in Figure 8. The administration of *HSE* at doses of 200 mg/kgBW and 400 mg/kgBW produced higher *Ucp-1* expression compared to that of the Ob group ($p <0.01$), reaching the normal levels.

4. Discussion

There was a higher *miR-34a* expression in the Ob group. This result is in line with that of Ahmadpour et al. (2018), who found an increase in the *miR-34a* expression in DIO rats [17]. Increased relative expression of *miR-34a* in the white adipose tissue during obesity has a relationship with adipogenesis. Some miRNAs, along with other adipogenesis master regulators, such as Peroxisome proliferator-activated receptor gamma (PPARγ) and CCAT-enhancer-binging proteins (C/EBP), increase the transcription of

adipogenic genes. According to Francisco (2010), *miR-34a* upregulation is followed by an increase of pre-adipocyte differentiation gene expression, while downregulation of *miR-34a* decreases the adipogenic gene expression [18].

Increased miR-34a causes chronic inflammation [3]. miR-34a plays a role in suppressing the expression of *Kruppel-like factor* 4 (*Klf4)*, which causes macrophage infiltration[3]. Macrophage infiltration is associated with an increase in TNF-α, which causes chronic inflammation. TNFα produced by macrophages plays an essential role in the regulation of adipokines in adipocytes. TNF-α induces proinflammatory cytokines through nuclear factor kappa B (NFκB). The binding of TNF-α to its receptor induces the production of proinflammatory cytokines through NFκB-dependent and -independent mechanisms. It also causes the production of proinflammatory cytokines, such as IL-Iβ, and IL-6 [19–21].

In this study, we did not measure the inflammatory cytokines in DIO rats. However, we showed the effects of *miR-34a* expression, as evidenced by decreased *Fgfr* and *Klb* expression. This study is in line with the work of Gallego-Escuredo (2015), who reported that obesity leads to the reduced expression of FGFR and beta-klotho receptors in the white adipose tissue [22]. Hale (2012) stated that the expression of beta-klotho, Fgfr-1c, and Fgfr2c are downregulated in the adipose tissue of DIO rats [23]. Delfin et al. (2012) found decreased expression of Fgfr1 and co-receptor beta-klotho in DIO rats. The decrease in the receptor numbers reduces the amount of binding with Fgf21. This decrease is supported by our previous research, which showed that the levels of Fgf21 expression in white adipose tissue in DIO mice are lower than that of the control group [24].

The decreased expression has an impact on endocrine Fgf21 communication in the adipose tissue and is the beginning of the development of Fgf21 resistance [19]. Fgf21 resistance leads to an increase in Fgf21 secretion in the liver [24]. The results of previous studies have shown that the expression of Fgf21 in the liver of the DIO rats is higher compared to the normal group. Increased expression levels of Fgf21 in the liver are a result of the disruption of Fgf21 uptake in the white adipose tissue. This happens as a compensation effect due to Fgf21 resistance. The increase in Fgf21 expression in the liver is followed by an increase in circulation [24]. Our results are in line with those of Geng et al. (2019), who found that serum Fgf21 levels in the DIO rats are six times higher than that in the normal group [18]. Research by Morrice et al. (2017) showed an increase in Fgf21 expression levels in the liver in mice with Fgf21 resistance [25].

The current study showed that the administration of HSE could manage Fgf21 resistance through increased expression of *Fgfr* and *Klb* [26]. *H. sabdariffa* is suggested to suppress miR-34a as a regulator of FGFR and beta-klotho expressions [27, 28]. However, the mechanism of how HSE downregulates miR-34a has not been proven. Several studies showed the potential of polyphenol compounds in other plant extracts that are microRNA modulators. Baselga-Escudero et al. (2015) showed that proanthocyanin, a component of polyphenols found in grapes and cocoa, downregulates miR-33. It also suppresses miR-122, which inhibits lipogenesis. Meanwhile, polyphenols from HSE modulate miR-122, miR-103, and miR-107 in hyperlipidemic rats [29].

The potential of HSE in suppressing miR-34a has been suggested through PPARγ and C/EBP expression. Additionally, a decrease in PPARγ and C/EBP expression is associated with miR-34a suppression. According to Lavery (2016), there is a decrease in the expression of Pparγ and C/EBP in miR-34a knockout rats [28]. According to Kim (2007), HSE suppresses transcription factors PPARγ and CEBP/α [30]. Thus, the inhibition of PPARγ and C/EBP as a result of HSE administration has the potential to suppress the expression of miR-34a [31].

However, suppressing the expression of miR-34a through the administration of HSE is related to the dose. Here, we showed that the administration of HSE at a dose of 200 mg/kg in DIO rats did not demonstrate a significant reduction in *miR-34a* expression compared to the Ob group. In contrast, the administration of HSE at a dose of 400 mg/kgBW was found to significantly reduce the expression of *miR-34* compared to that of the Ob group. Even though miR-34 expression levels do not reach normal levels, beta-klotho and FGFR expression can still increase [32], reaching normal levels of FGFR1 expression.

The increased expression of beta-klotho and FGFR can also be influenced by HSE, which directly suppresses chronic inflammation. Some studies have found that polyphenols in the HSE can inhibit proinflammation by suppressing NFκB. Zeng et al. (2016) found that polyphenols increase the expression of Fgfr1 and beta-klotho in rats fed with a high-fat diet [33]. This is because polyphenols act as anti-inflammatory agents by decreasing NFκB expression. The results of Gamboa-Gomez (2015) indicate that HSE significantly reduces TNFα induced by NFκB [34]. In addition, the anthocyanins, namely cyanidin and delphinidin, in the HSE, also reduce TNFα expression. That is because anthocyanin inhibits the activation of NFκB by inhibiting the degradation of IκB and inhibiting the activation of IκB kinase, thereby preventing the phosphorylation of NFκB [19]. In the current study, we did not measure NFκB expression levels; thus, we could not directly prove that the increase in *Klb* and *Fgfr* expression was associated with a decrease in NFκB. This study proves the potential of HSE in increasing the expression of *Fgfr* and *Klb*, such that it can manage Fgf21 resistance in DIO rats [35].

Our previous research showed that there is a higher than normal increase in Fgf21 in the adipose tissue of DIO mice administered HSE at a dose of 400 mg/kgBW. The management of FGF21 resistance is indicated by the activation of the FGF21 signaling pathway in the adipose tissue. FGF21 binds with its receptor to activate signaling via PGC1α, which is a transcription coactivator that controls energy metabolism. The present study showed an increase in *Ppargc1a* expression in the Ob-Hib400 group.

SIRT1 stimulates increased PGC1α activity. After FGF21 binds to FGFR and beta-klotho, it induces browning of white adipose tissue to beige adipose tissue through SIRT1 activation, which results in PGC1α deacetylation to induce UCP-1 expression [5]. The results of the current study also showed an increase in *Ucp-1* expression after HSE administration. The rise in *Ucp-1* expression was shown not only in the Ob-Hib400 group but also in the Ob-Hib200 group.

The increase in UCP-1 expression is not only affected by PGC1α activation but also by other factors [33]. UCP-1 expression is influenced by several paths that are regulated by major transcription factors, such as

PPARγ and PRDM16 [36].

PPARγ is a crucial transcription factor in the differentiation of brown and white adipocytes. PPARγ is needed for the recruitment of PRDM16 to the PPARγ transcription complex, which achieves the browning process [37]. Thus, HSE not only activates the PGC1α pathway but is also thought to play a role in the PPARγ and PRDM16 pathways. However, further research is needed to prove this. According to Tian (2017), polyphenol content from green tea improves transcriptional regulators, such as PPARγ, PGC1α, PRDM16, and UCP1, for the browning process [38].

5. Conclusion

H. sabdariffa has the potential to manage Fgf21 resistance in DIO rats via the suppression of *miR-34a* expression, increasing the number of Fgfr1 and beta-klotho co-receptors in the adipose tissue. This condition affects active FGF21 signaling in the process of browning and thermogenesis.

Abbreviations

Fgf 21
Fibroblast growth factor 21
Fgfr21
Fibroblast growth factor receptor 21
miR-34a
microRNA 34a
HSE
Hibiscus sabdariffa Linn extract
DIO
diet-induced-obesity rats
TNFα
tumor necrosis factor alpha
SIRT1
Sirtuin-1
PGC1α
Peroxisome proliferator-activated receptor-gamma coactivator
UCP-1
uncoupling protein 1
CHOD-PAP
Cholesterol Oxidase-Peroxidase Aminoantypirin)
PPARγ
Peroxisome proliferator-activated receptor gamma
C/EBP
CCAT-enhancer-binging proteins

Klf4
Kruppel-like factor 4
NFκB
nuclear factor kappa B
Klb
Klotho beta
PRDM16
PR domain containing 16

Declarations

1. **Ethics approval**: The Ethical Committee of Faculty of Medicine, Universitas Indonesia approved all experiments, with No: 0110/UN@.F1.ETIK/2018

Consent for participation: Not applicable (samples using animal tissue)

2. **Consent for publication**: Not applicable (samples using animal tissue)
3. **Availability of data and material:** The datasets during and/or analysed during the current study available from the corresponding author on reasonable request
4. **Competing interests:** The authors declare that they have no competing interests.
5. **Funding:** The research was funded by Ministry of Research, Technology, and Higher Education who provide the research Grant with contract No. NKB-1547/UN2.R3.1/HKP.05.00/2019.
6. **Authors' contributions**

Conceived and designed the experiment: NTK, IRS. Performed the experiments: NK, NN, AR, H. Analyzed the data: NTK, AR, IRS. Contributed reagents/materials/analysis tools: NK, NTK, AR,SY. Wrote the paper: SY, NTK, IRS. Commented on the manuscript before submission: NTK, IRS.

7. **Acknowledgments**

The authors would like to thank the Ministry of Research, Technology, and Higher Education who provide the research Grant with contract No. NKB-1547/UN2.R3.1/HKP.05.00/2019.

References

1. Pan Y, Hui X, Hoo RLC, Ye D, Chan CYC, Feng T, et al. Adipocyte-secreted exosomal microRNA-34a inhibits M2 macrophage polarization to promote obesity-induced adipose inflammation. J Clin Invest. 2019;129(2):834-49. DOI: 10.1172/JCI123069
2. Balasubramaniam M, Pandhare J, Dash C. Are microRNAs important players in HIV-1 infection? An update. Viruses. 2018;10(3). DOI: 10.3390/v10030110

3. Fu T, Seok S, Choi S, Huang Z, Suino-Powell K, Xu HE, et al. MicroRNA 34a inhibits beige and brown fat formation in obesity in part by suppressing adipocyte fibroblast growth factor 21 signaling and SIRT1 function. Mol Cell Biol. 2014;34(22):4130-42. DOI: 10.1128/MCB.00596-14
4. Fisher FM, Kleiner S, Douris N, Fox EC, Mepani RJ, Verdeguer F, et al. FGF21 regulates PGC-1alpha and browning of white adipose tissues in adaptive thermogenesis. Genes Dev. 2012;26(3):271-81. DOI: 10.1101/gad.177857.111
5. Crichton PG, Lee Y, Kunji ER. The molecular features of uncoupling protein 1 support a conventional mitochondrial carrier-like mechanism. Biochimie. 2017;134:35-50. DOI: 10.1016/j.biochi.2016.12.016
6. Tine Kartinah N, Rosalyn Sianipar I, Nafi'ah, Rabia. The effects of exercise regimens on Irisin levels in obese rats model: Comparing high-intensity intermittent with continuous moderate-intensity training. Biomed Res Int. 2018;2018:4708287. https://doi.org/10.1155/2018/4708287
7. Sonoda J, Chen MZ, Baruch A. FGF21-receptor agonists: an emerging therapeutic class for obesity-related diseases. Horm Mol Biol Clin Investig. 2017;30(2). DOI: 10.1515/hmbci-2017-0002
8. Riaz G, Chopra R. A review on phytochemistry and therapeutic uses of Hibiscus sabdariffa L. Biomed Pharmacother. 2018;102:575-86. DOI: 10.1016/j.biopha.2018.03.023
9. Morales-Luna E, Perez-Ramirez IF, Salgado LM, Castano-Tostado E, Gomez-Aldapa CA, Reynoso-Camacho R. The main beneficial effect of roselle (Hibiscus sabdariffa) on obesity is not only related to its anthocyanin content. J Sci Food Agric. 2019;99(2):596-605. DOI: 10.1002/jsfa.9220
10. Guardiola S, Mach N. [Therapeutic potential of Hibiscus sabdariffa: a review of the scientific evidence]. Endocrinol Nutr. 2014;61(5):274-95. DOI: 10.1016/j.endonu.2013.10.012
11. Herranz-Lopez M, Olivares-Vicente M, Encinar JA, Barrajon-Catalan E, Segura-Carretero A, Joven J, et al. Multi-targeted molecular effects of Hibiscus sabdariffa polyphenols: An opportunity for a global approach to obesity. Nutrients. 2017;9(8). DOI: 10.3390/nu9080907
12. Tuncer GO, Koker A, Koker SA, Aba A, Kara TT, Coban Y, et al. Infantile tremor syndrome after peroral and intramuscular vitamin B12 therapy: Two Cases. Klin Padiatr. 2019. DOI: 10.1055/a-0981-6355
13. Marques C, Meireles M, Norberto S, Leite J, Freitas J, Pestana D, et al. High-fat diet-induced obesity Rat model: a comparison between Wistar and Sprague-Dawley Rat. Adipocyte. 2016;5(1):11-21. DOI: 10.1080/21623945.2015.1061723
14. Jamali E, Asad M, Rassouli A. The effect of high-intensity training (HIIT) on resistin gene expression in visceral adipose tissue in obese male rats. International Journal of Applied Exercise Physiology. 2016;5(1):17-25. http://www.ijaep.com/index.php/IJAE/article/view/40
15. Andraini T, Yolanda S. Prevention of insulin resistance with Hibiscus sabdariffa Linn. extract in high-fructose fed rat. Med J Indones. 2014;23(4):192-6. https://doi.org/10.13181/mji.v23i4.848
16. Baselga-Escudero L, Pascual-Serrano A, Ribas-Latre A, Casanova E, Salvado MJ, Arola L, et al. Long-term supplementation with a low dose of proanthocyanidins normalized liver miR-33a and miR-122 levels in high-fat diet-induced obese rats. Nutr Res. 2015;35(4):337-45. DOI: 10.1016/j.nutres.2015.02.008

17. Ahmadpour F, Nourbakhsh M, Razzaghy-Azar M, Khaghani S, Alipoor B, Abdolvahabi Z, et al. The Association of plasma levels of miR-34a and miR-149 with obesity and insulin resistance in obese children and adolescents. Acta Endocrinol (Buchar). 2018;14(2):149-54. DOI: 10.4183/aeb.2018.149
18. Cuevas-Ramos D, Almeda-Valdes P, Meza-Arana CE, Brito-Cordova G, Gomez-Perez FJ, Mehta R, et al. Exercise increases serum fibroblast growth factor 21 (FGF21) levels. PLoS One. 2012;7(5):e38022. DOI: 10.20463/jenb.2017.0008
19. Diaz-Delfin J, Hondares E, Iglesias R, Giralt M, Caelles C, Villarroya F. TNF-alpha represses beta-Klotho expression and impairs FGF21 action in adipose cells: involvement of JNK1 in the FGF21 pathway. Endocrinology. 2012;153(9):4238-45. DOI: 10.1210/en.2012-1193
20. McArdle MA, Finucane OM, Connaughton RM, McMorrow AM, Roche HM. Mechanisms of obesity-induced inflammation and insulin resistance: insights into the emerging role of nutritional strategies. Front Endocrinol (Lausanne). 2013;4:52. DOI: 10.3389/fendo.2013.00052
21. Wang X, Cheng M, Zhao M, Ge A, Guo F, Zhang M, et al. Differential effects of high-fat-diet rich in lard oil or soybean oil on osteopontin expression and inflammation of adipose tissue in diet-induced obese rats. Eur J Nutr. 2013;52(3):1181-9. DOI: 10.1007/s00394-012-0428-z
22. Gallego-Escuredo JM, Gomez-Ambrosi J, Catalan V, Domingo P, Giralt M, Fruhbeck G, et al. Opposite alterations in FGF21 and FGF19 levels and disturbed expression of the receptor machinery for endocrine FGFs in obese patients. Int J Obes (Lond). 2015;39(1):121-9. DOI: 10.1038/ijo.2014.76
23. Hale C, Chen MM, Stanislaus S, Chinookoswong N, Hager T, Wang M, et al. Lack of overt FGF21 resistance in two mouse models of obesity and insulin resistance. Endocrinology. 2012;153(1):69-80. DOI: 10.1210/en.2010-1262
24. Kartinah N, Komara N, Sianipar I, Noviati N. The potential of Hibiscus sabdariffa for treatment of obesity: Focus on FGF 21 in liver and adipose tissue. eJKI. 2019;7(2):131-6. https://doi/org/10.23886/ejki.7.11093.
25. Hondares E, Iglesias R, Giralt A, Gonzalez FJ, Giralt M, Mampel T, et al. Thermogenic activation induces FGF21 expression and release in brown adipose tissue. J Biol Chem. 2011;286(15):12983-90. DOI: 10.1074/jbc.M110.215889
26. BonDurant LD, Ameka M, Naber MC, Markan KR, Idiga SO, Acevedo MR, et al. FGF21 regulates metabolism through adipose-dependent and -independent mechanisms. Cell Metab. 2017;25(4):935-44 e4. https://doi.org/10.1016/j.cmet.2017.03.005
27. Shi C, Huang F, Gu X, Zhang M, Wen J, Wang X, et al. Adipogenic miRNA and meta-signature miRNAs involved in human adipocyte differentiation and obesity. Oncotarget. 2016;7(26):40830-45. DOI: 10.18632/oncotarget.8518
28. Lavery CA, Kurowska-Stolarska M, Holmes WM, Donnelly I, Caslake M, Collier A, et al. miR-34a(-/-) mice are susceptible to diet-induced obesity. Obesity (Silver Spring). 2016;24(8):1741-51. DOI: 10.1002/oby.21561
29. Yang Z, Cappello T, Wang L. Emerging role of microRNAs in lipid metabolism. Acta Pharm Sin B. 2015;5(2):145-50. DOI: 10.1016/j.apsb.2015.01.002

30. Kim MS, Kim JK, Kim HJ, Moon SR, Shin BC, Park KW, et al. Hibiscus extract inhibits the lipid droplet accumulation and adipogenic transcription factors expression of 3T3-L1 preadipocytes. J Altern Complement Med. 2003;9(4):499-504. DOI: 10.1089/107555303322284785
31. Hausman GJ, Basu U, Wei S, Hausman DB, Dodson MV. Preadipocyte and adipose tissue differentiation in meat animals: influence of species and anatomical location. Annu Rev Anim Biosci. 2014;2:323-51. DOI: 10.1146/annurev-animal-022513-114211
32. Agrawal A, Parlee S, Perez-Tilve D, Li P, Pan J, Mroz PA, et al. Molecular elements in FGF19 and FGF21 defining KLB/FGFR activity and specificity. Mol Metab. 2018;13:45-55. DOI: 10.1016/j.molmet.2018.05.003
33. Zeng K, Tian L, Patel R, Shao W, Song Z, Liu L, et al. Diet polyphenol curcumin stimulates hepatic Fgf21 production and restores its sensitivity in high-fat-diet-fed male mice. Endocrinology. 2017;158(2):277-92. DOI: 10.1210/en.2016-1596
34. Gamboa-Gomez CI, Rocha-Guzman NE, Gallegos-Infante JA, Moreno-Jimenez MR, Vazquez-Cabral BD, Gonzalez-Laredo RF. Plants with potential use on obesity and its complications. EXCLI J. 2015;14:809-31. DOI: 10.17179/excli2015-186
35. Fisher FM, Chui PC, Antonellis PJ, Bina HA, Kharitonenkov A, Flier JS, et al. Obesity is a fibroblast growth factor 21 (FGF21)-resistant state. Diabetes. 2010;59(11):2781-9. DOI: 10.2337/db10-0193
36. Lo KA, Sun L. Turning WAT into BAT: a review on regulators controlling the browning of white adipocytes. Biosci Rep. 2013;33(5). DOI: 10.1042/BSR20130046
37. Xie Q, Tian T, Chen Z, Deng S, Sun K, Xie J, et al. Peroxisome proliferator-activated receptor (PPAR) in regenerative medicine: Molecular mechanism for PPAR in stem cells' adipocyte differentiation. Curr Stem Cell Res Ther. 2016;11(3):290-8. DOI: 10.2174/1574888x10666150902093755
38. Tian C, Ye X, Zhang R, Long J, Ren W, Ding S, et al. Green tea polyphenols reduced fat deposits in high fat-fed rats via erk1/2-PPARgamma-adiponectin pathway. PLoS One. 2013;8(1):e53796. DOI: 10.1371/journal.pone.0053796

Figures

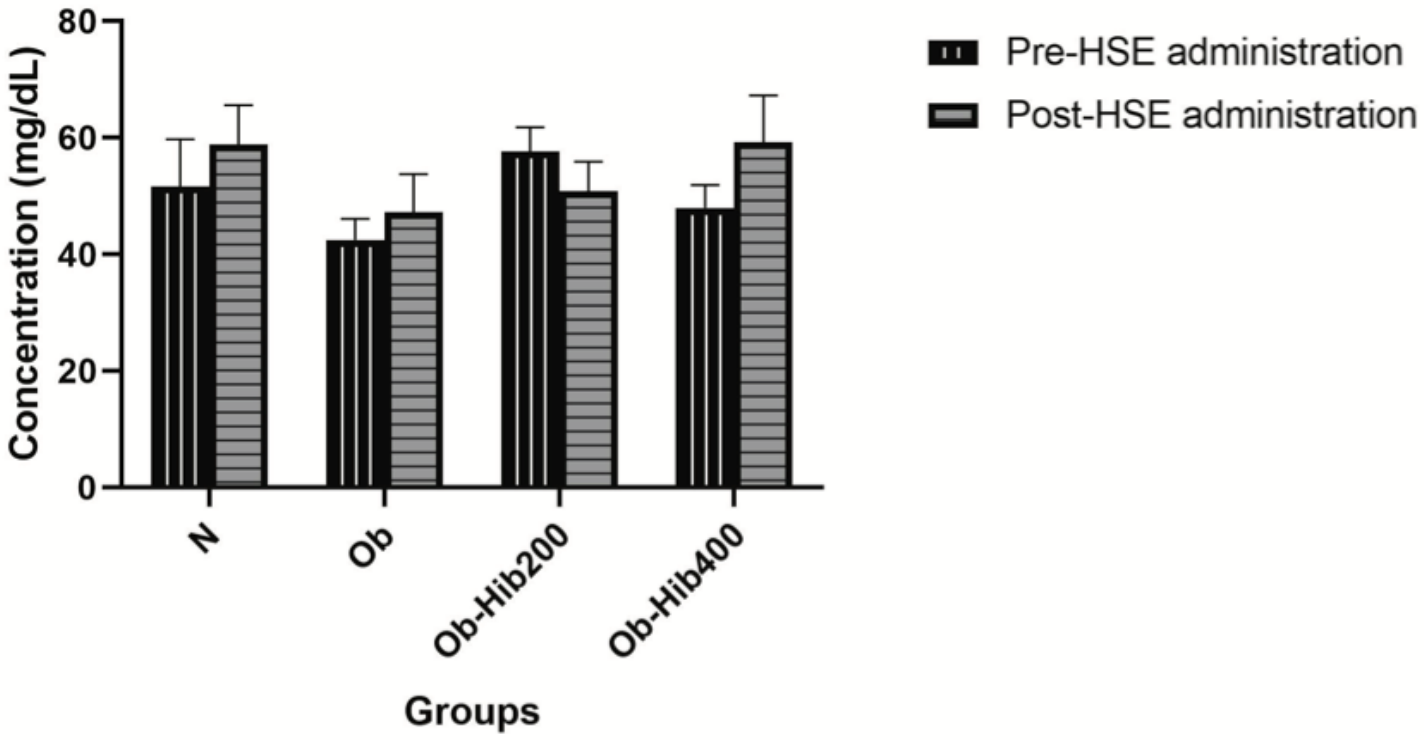

Figure 1

Total cholesterol concentration pre- and post-HSE administration Data are depicted as mean ± SD. Significant differences are shown as *p<0.05. N: Normal control group; Ob: DIO rats; Ob-Hib 200: DIO rats administered with H. sabdariffa (HSE) at a dose of 200 mg/kgBW; Ob-Hib 400: DIO rats administered with HSE at a dose of 400 mg/kgBW; SD: standard deviation, HSE: H. Sabdariffa.

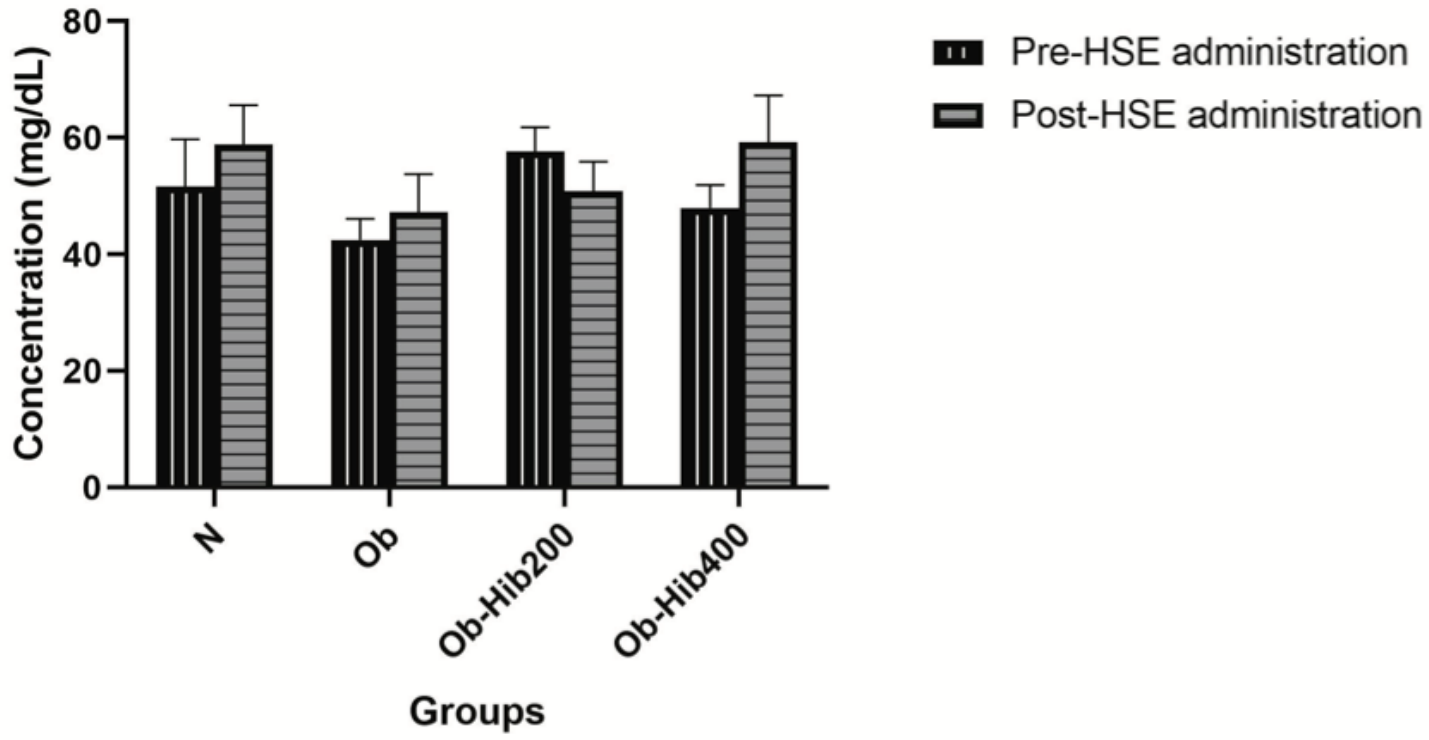

Figure 1

Total cholesterol concentration pre- and post-HSE administration Data are depicted as mean ± SD. Significant differences are shown as *p<0.05. N: Normal control group; Ob: DIO rats; Ob-Hib 200: DIO rats administered with H. sabdariffa (HSE) at a dose of 200 mg/kgBW; Ob-Hib 400: DIO rats administered with HSE at a dose of 400 mg/kgBW; SD: standard deviation, HSE: H. Sabdariffa.

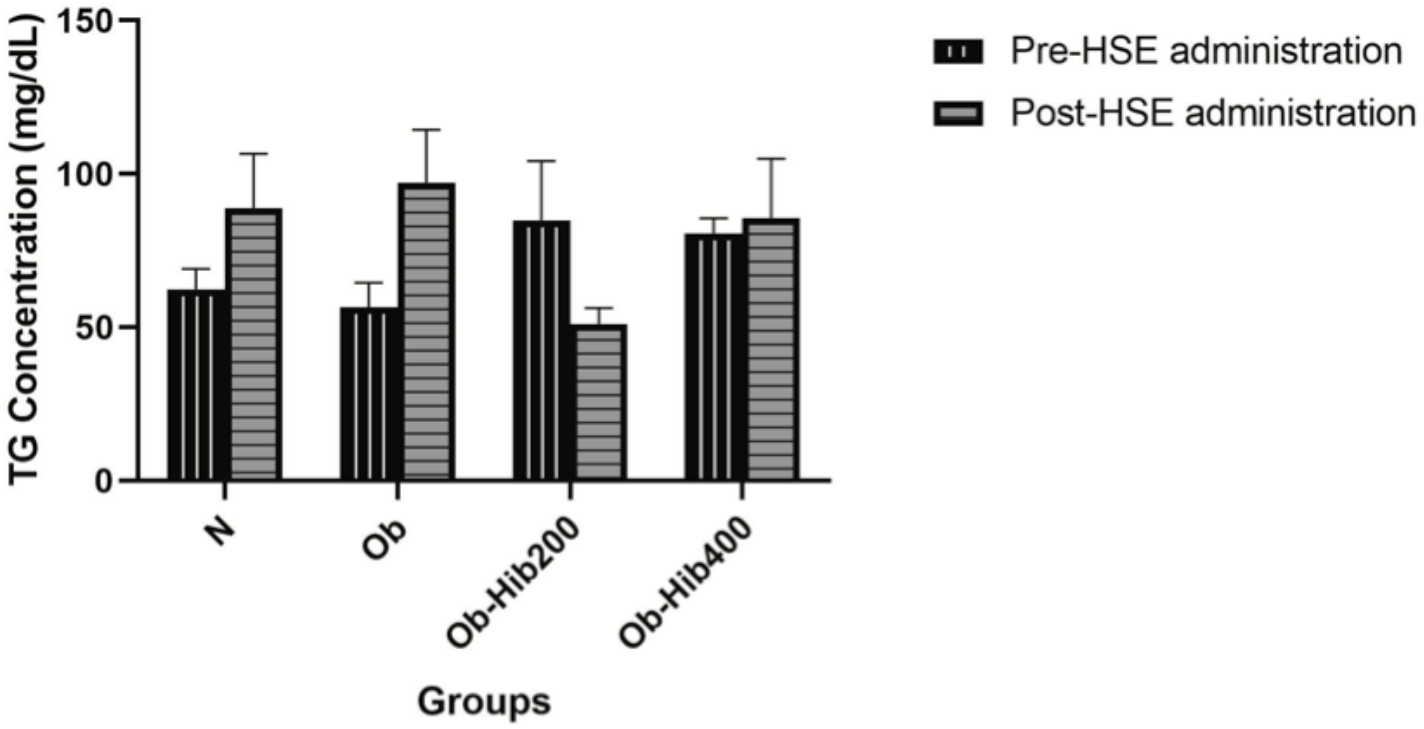

Figure 2

Triglyceride concentration pre- and post-HSE administration Data are depicted as mean ± SD. Significant differences are shown as *p<0.05. N: Normal control group; Ob: DIO rats; Ob-Hib 200: DIO rats administered with HSE at a dose of 200 mg/kgBW; Ob-Hib 400: DIO rats administered with HSE at a dose of 400 mg/kgBW; SD: standard deviation, HSE: H. Sabdariffa.

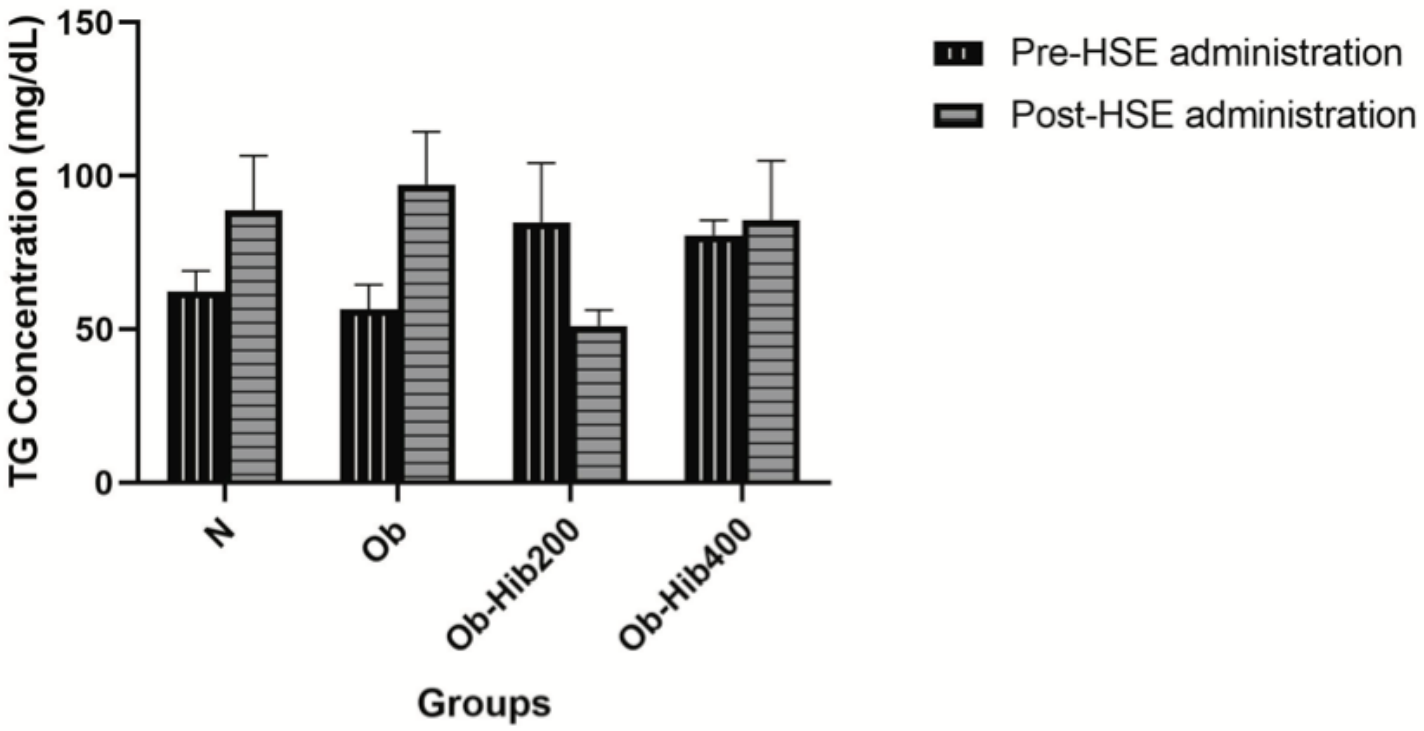

Figure 2

Triglyceride concentration pre- and post-HSE administration Data are depicted as mean ± SD. Significant differences are shown as *p<0.05. N: Normal control group; Ob: DIO rats; Ob-Hib 200: DIO rats administered with HSE at a dose of 200 mg/kgBW; Ob-Hib 400: DIO rats administered with HSE at a dose of 400 mg/kgBW; SD: standard deviation, HSE: H. Sabdariffa.

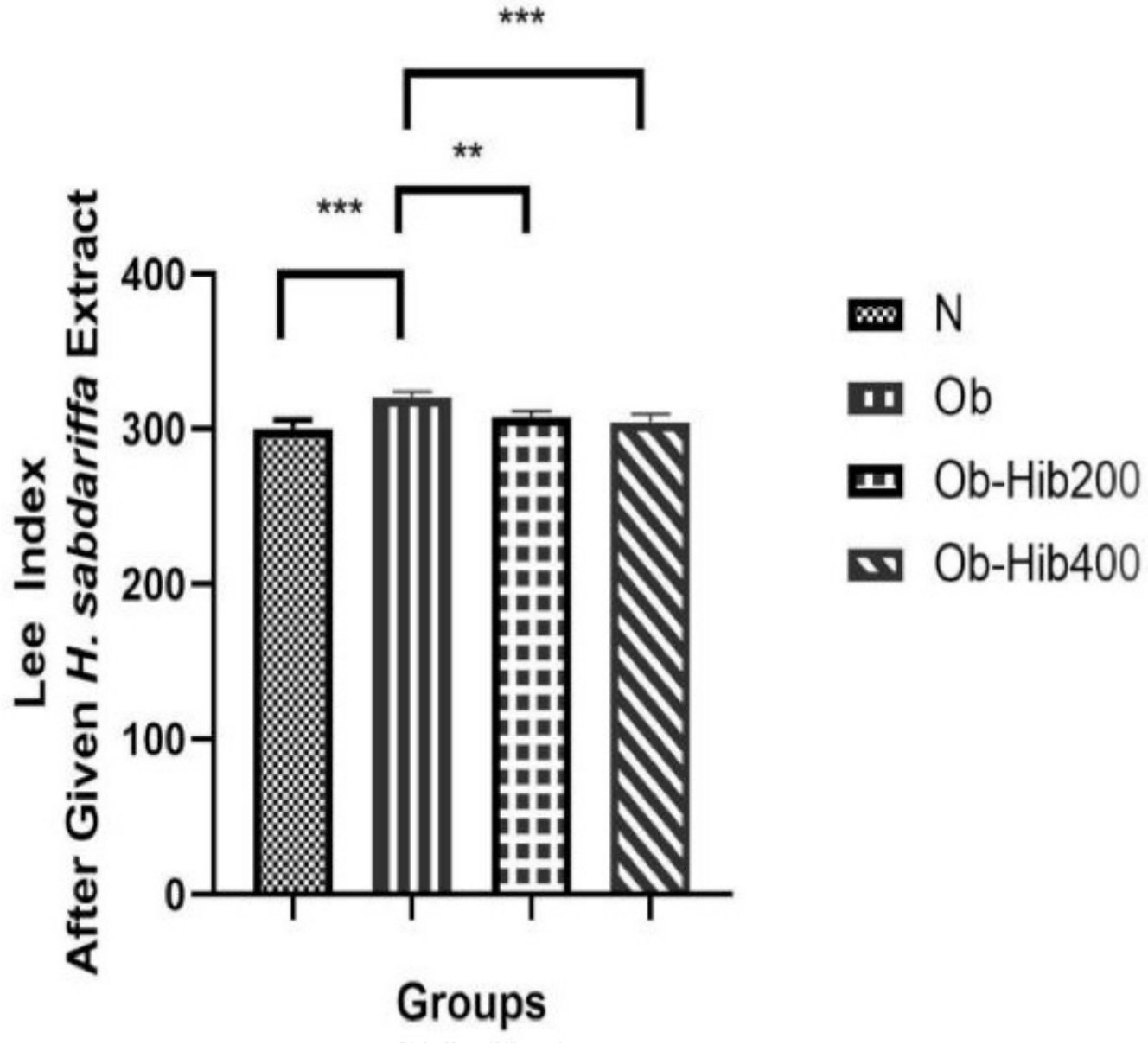

Figure 3

Average Lee index Data are depicted as mean ± SD. Significant differences are shown as *p<0.05, **p<0.01, ***p<0.001; N: Normal control group; Ob: DIO rats; Ob-Hib 200: DIO rats administered with HSE at a dose of 200 mg/kgBW; Ob-Hib 400: DIO rats administered with HSE at a dose of 400 mg/kgBW; SD: standard deviation, HSE: H. Sabdariffa.

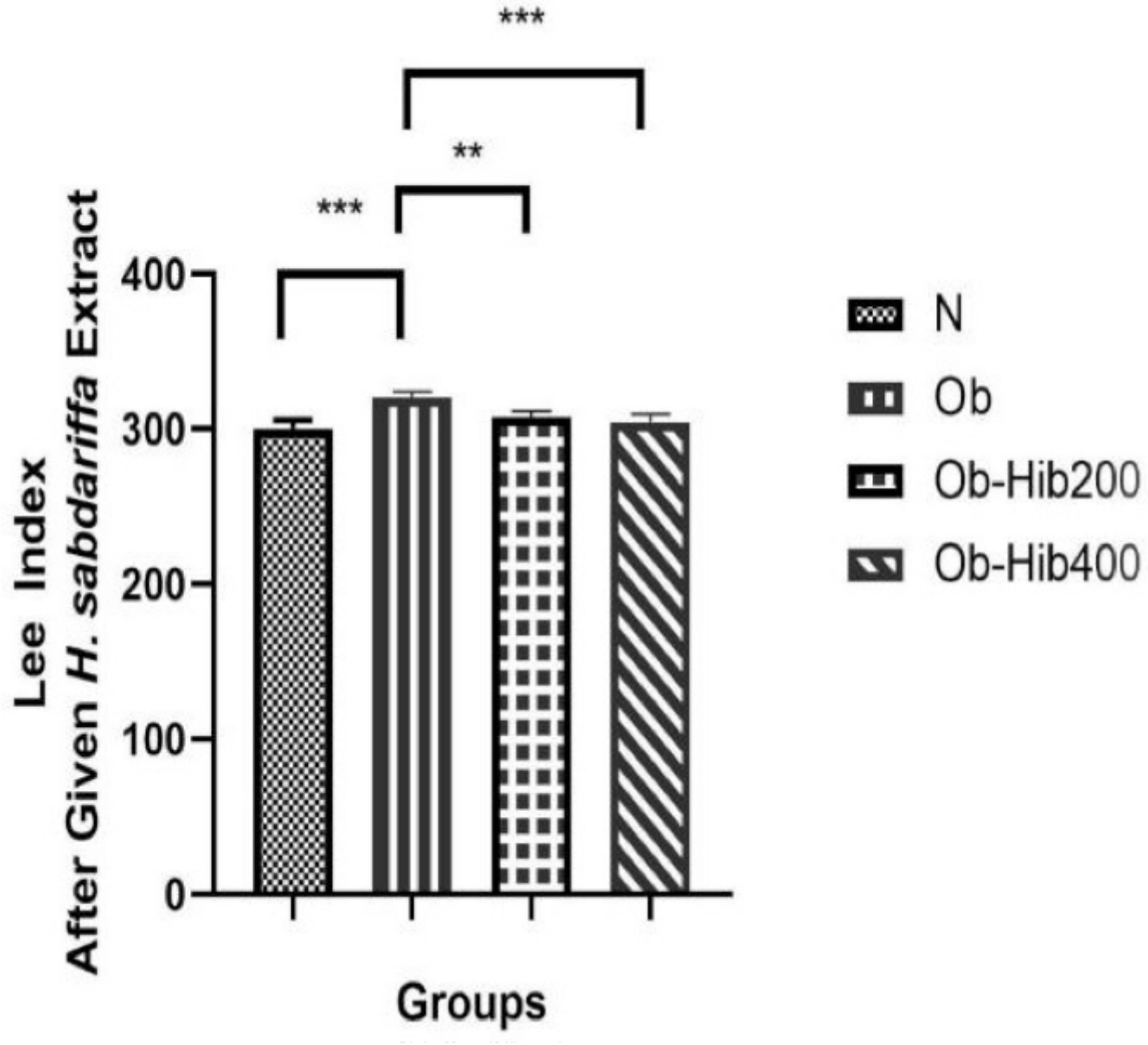

Figure 3

Average Lee index Data are depicted as mean ± SD. Significant differences are shown as *p<0.05, **p<0.01, ***p<0.001; N: Normal control group; Ob: DIO rats; Ob-Hib 200: DIO rats administered with HSE at a dose of 200 mg/kgBW; Ob-Hib 400: DIO rats administered with HSE at a dose of 400 mg/kgBW; SD: standard deviation, HSE: H. Sabdariffa.

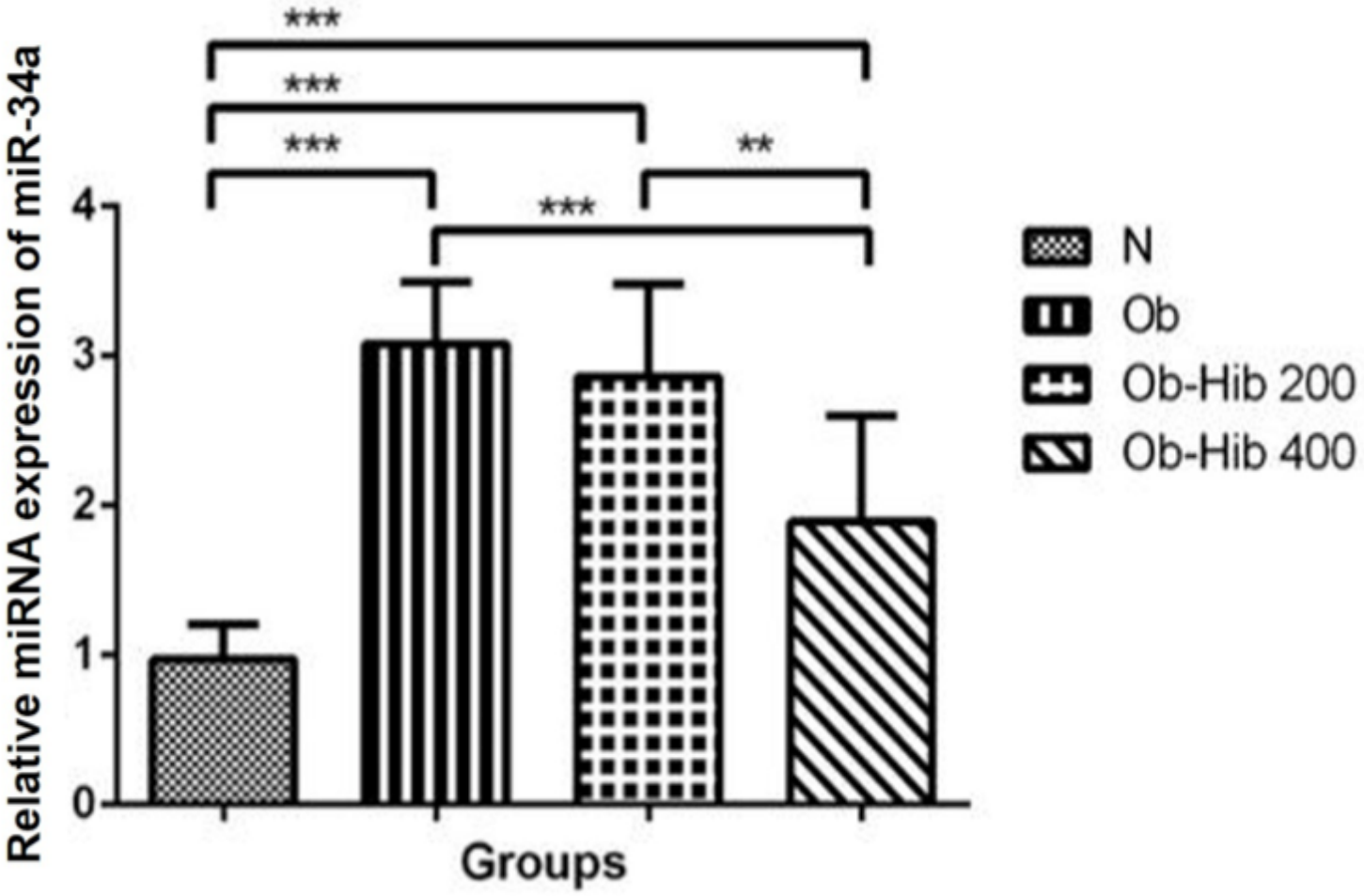

Figure 4

Average miR-34a expression Data are depicted as mean ± SD. Significant differences are shown as *p<0.05, **p<0.01, ***p<0.001. N: Normal control group; Ob: DIO rats; Ob-Hib 200: DIO rats administered with HSE at a dose of 200 mg/kgBW; Ob-Hib 400: DIO rats administered with HSE at a dose of 400 mg/kgBW; SD: standard deviation, HSE: H. Sabdariffa.

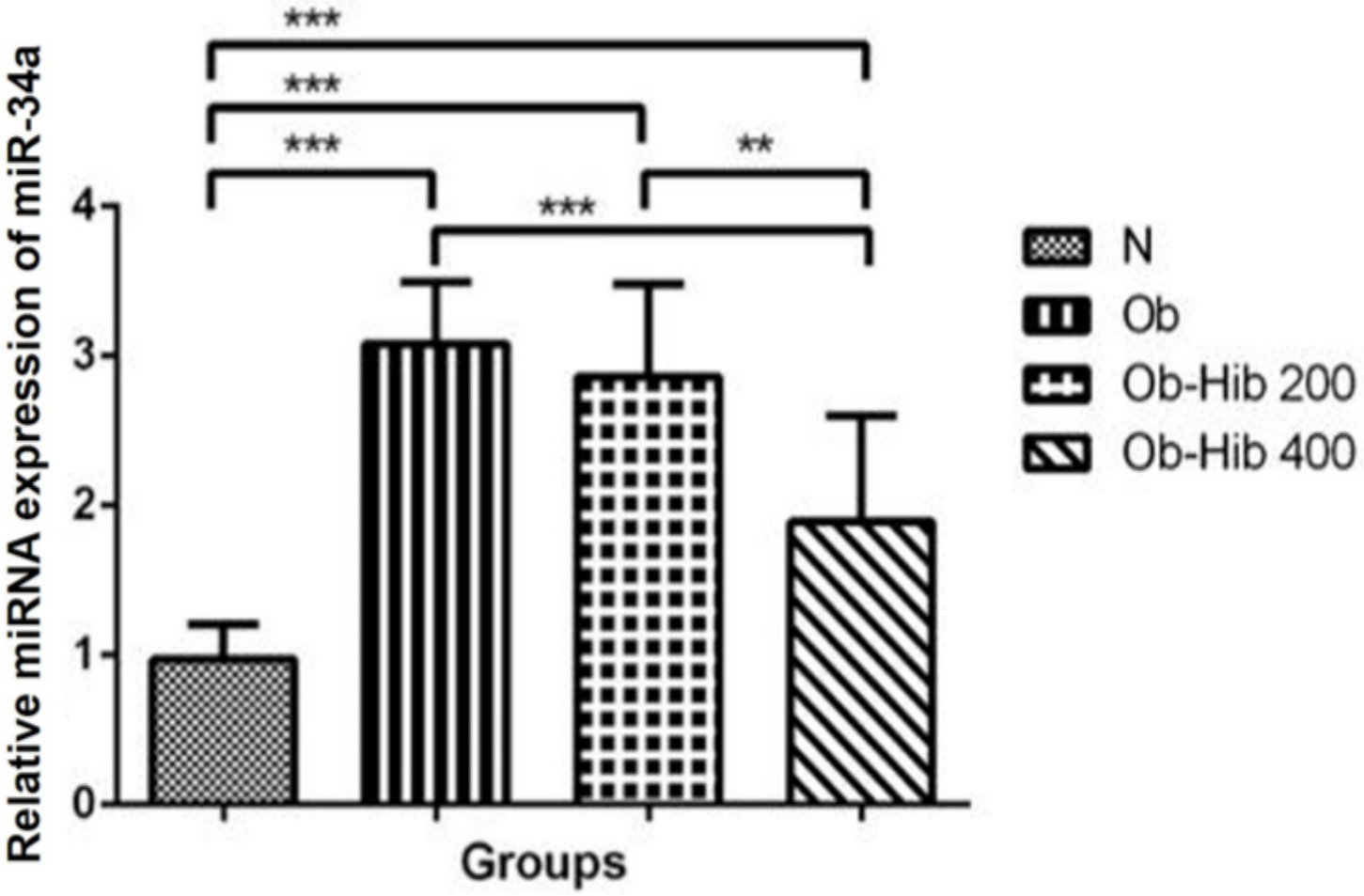

Figure 4

Average miR-34a expression Data are depicted as mean ± SD. Significant differences are shown as *p<0.05, **p<0.01, ***p<0.001. N: Normal control group; Ob: DIO rats; Ob-Hib 200: DIO rats administered with HSE at a dose of 200 mg/kgBW; Ob-Hib 400: DIO rats administered with HSE at a dose of 400 mg/kgBW; SD: standard deviation, HSE: H. Sabdariffa.

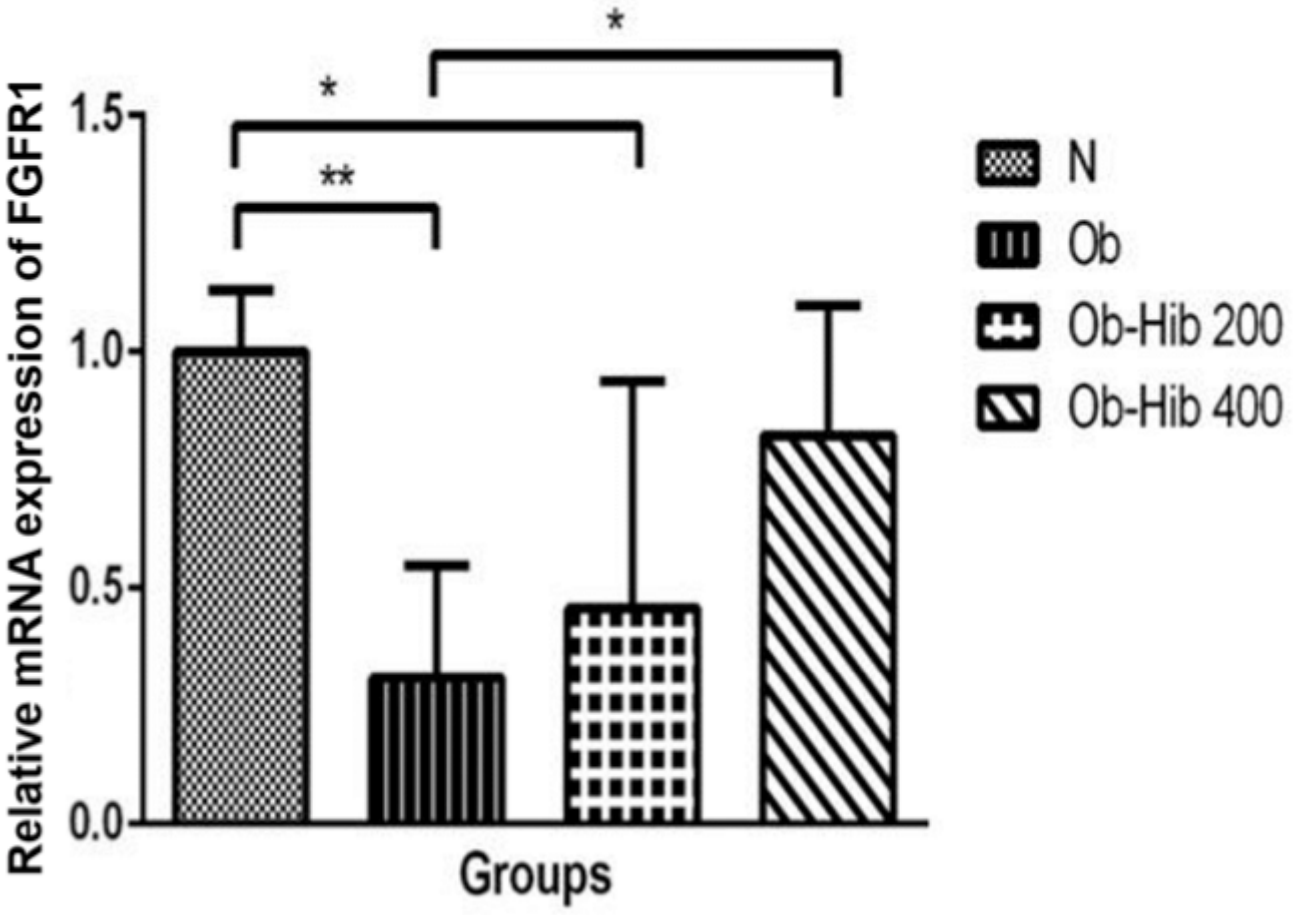

Figure 5

Average Fgfr1 expression Data are depicted as mean ± SD. Significant differences are shown as *p<0.05, **p<0.01, ***p<0.001. N: Normal control group; Ob: DIO rats; Ob-Hib 200: DIO rats administered with H. sabdariffa at a dose of 200 mg/kgBW; Ob-Hib 400: DIO rats administered with H. sabdariffa at a dose of 400 mg/kgBW; SD: standard deviation, HSE: H. Sabdariffa.

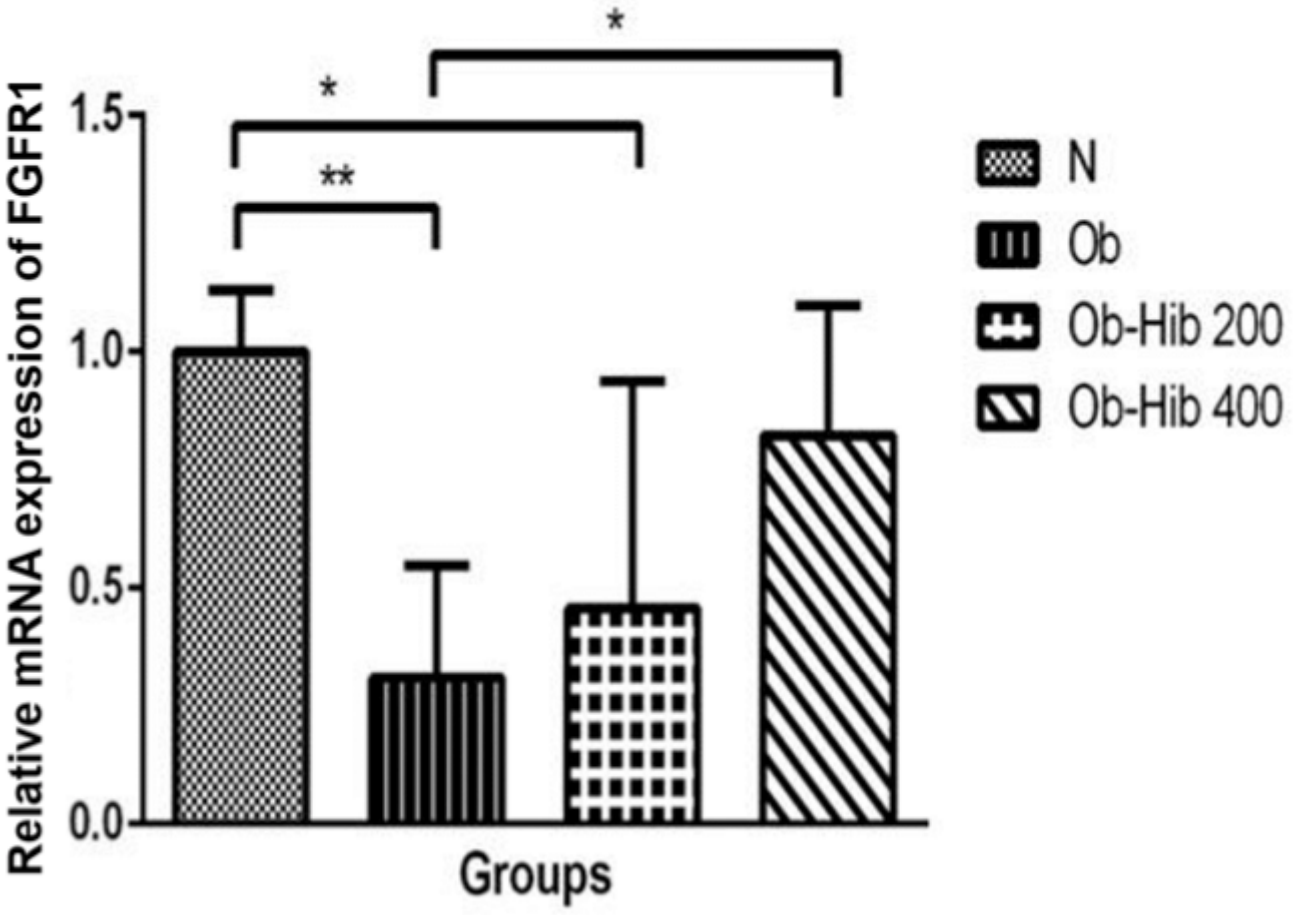

Figure 5

Average Fgfr1 expression Data are depicted as mean ± SD. Significant differences are shown as *p<0.05, **p<0.01, ***p<0.001. N: Normal control group; Ob: DIO rats; Ob-Hib 200: DIO rats administered with H. sabdariffa at a dose of 200 mg/kgBW; Ob-Hib 400: DIO rats administered with H. sabdariffa at a dose of 400 mg/kgBW; SD: standard deviation, HSE: H. Sabdariffa.

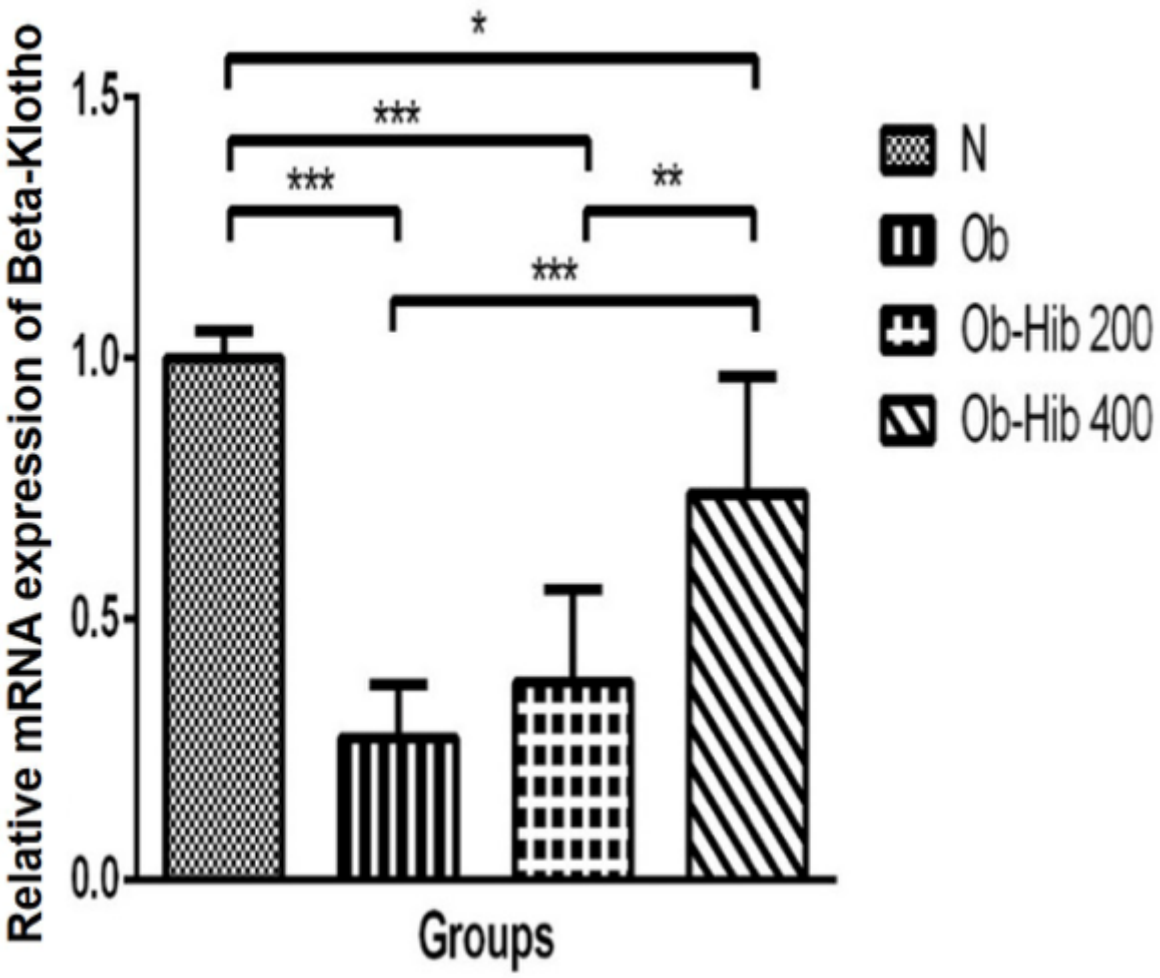

Figure 6

Average Klb expression Data are depicted as mean ± SD. Significant differences are shown as *p<0.05, **p<0.01, ***p<0.001. N: Normal control group; Ob: DIO rats; Ob-Hib 200: DIO rats administered with HSE at a dose of 200 mg/kgBW; Ob-Hib 400: DIO rats administered with HSE at a dose of 400 mg/kgBW; SD: standard deviation, HSE: H. Sabdariffa.

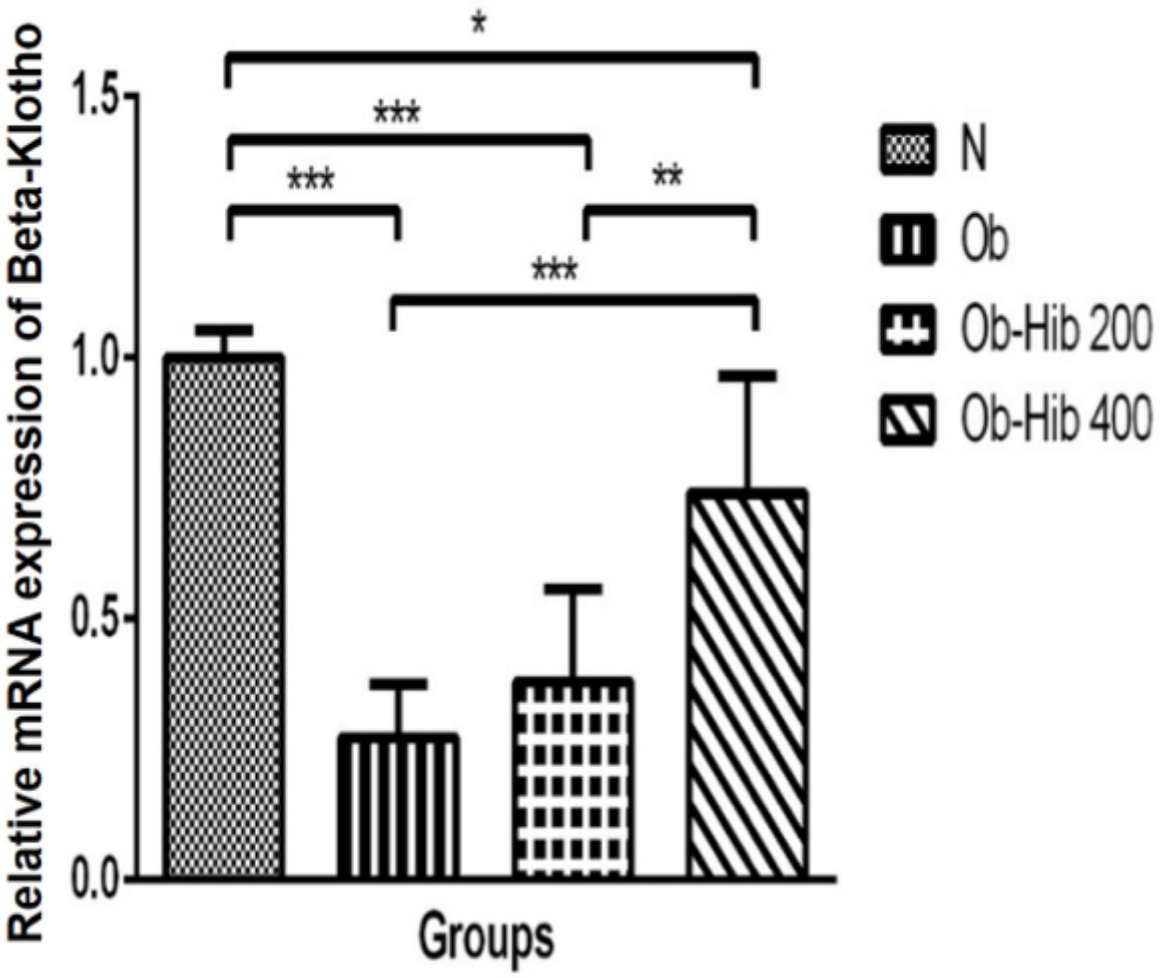

Figure 6

Average Klb expression Data are depicted as mean ± SD. Significant differences are shown as *p<0.05, **p<0.01, ***p<0.001. N: Normal control group; Ob: DIO rats; Ob-Hib 200: DIO rats administered with HSE at a dose of 200 mg/kgBW; Ob-Hib 400: DIO rats administered with HSE at a dose of 400 mg/kgBW; SD: standard deviation, HSE: H. Sabdariffa.

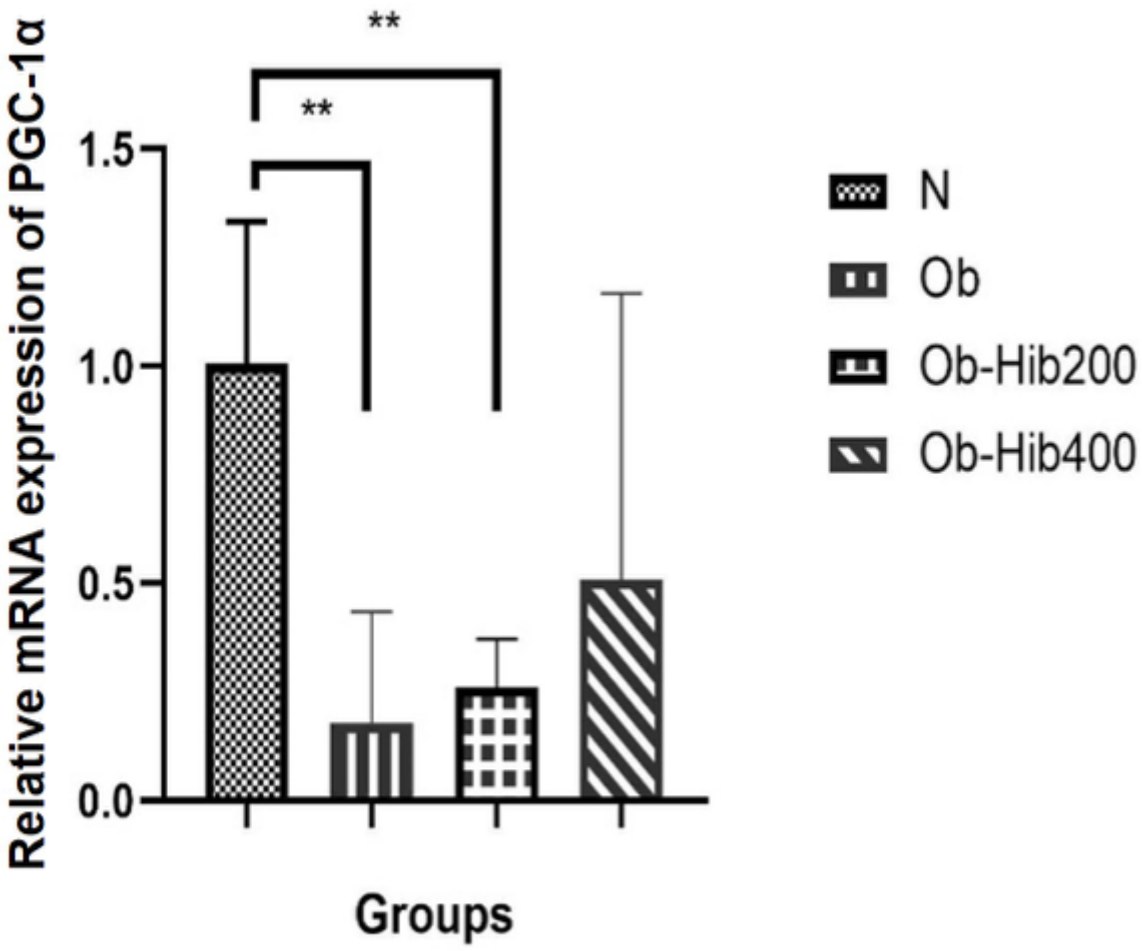

Figure 7

Average Ppargc1a expression Data are depicted as mean ± SD. Significant differences are shown as *p<0.05, **p<0.01, ***p<0.001. N: Normal control group; Ob: DIO rats; Ob-Hib 200: DIO rats administered with HSE at a dose of 200 mg/kgBW; Ob-Hib 400: DIO rats administered with HSE at a dose of 400 mg/kgBW; SD: standard deviation, HSE: H. Sabdariffa.

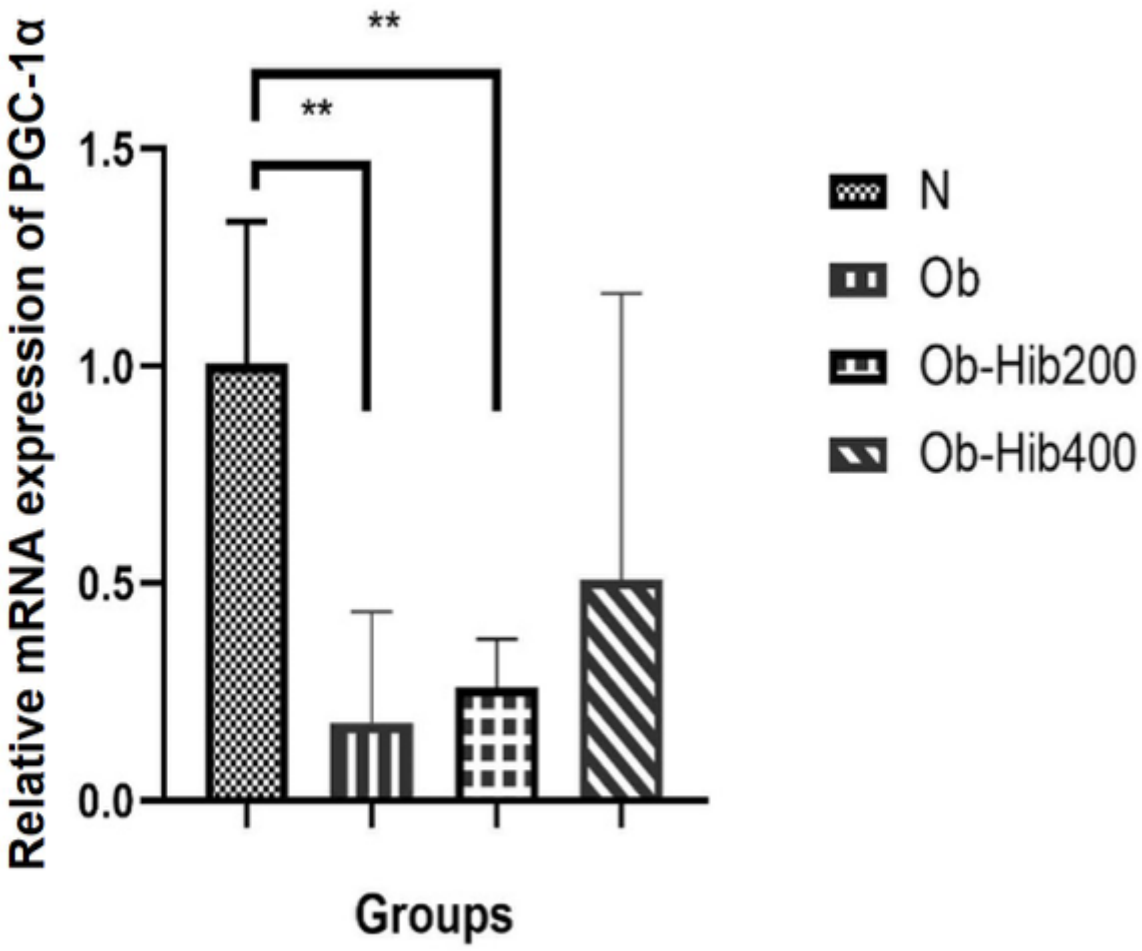

Figure 7

Average Ppargc1a expression Data are depicted as mean ± SD. Significant differences are shown as *p<0.05, **p<0.01, ***p<0.001. N: Normal control group; Ob: DIO rats; Ob-Hib 200: DIO rats administered with HSE at a dose of 200 mg/kgBW; Ob-Hib 400: DIO rats administered with HSE at a dose of 400 mg/kgBW; SD: standard deviation, HSE: H. Sabdariffa.

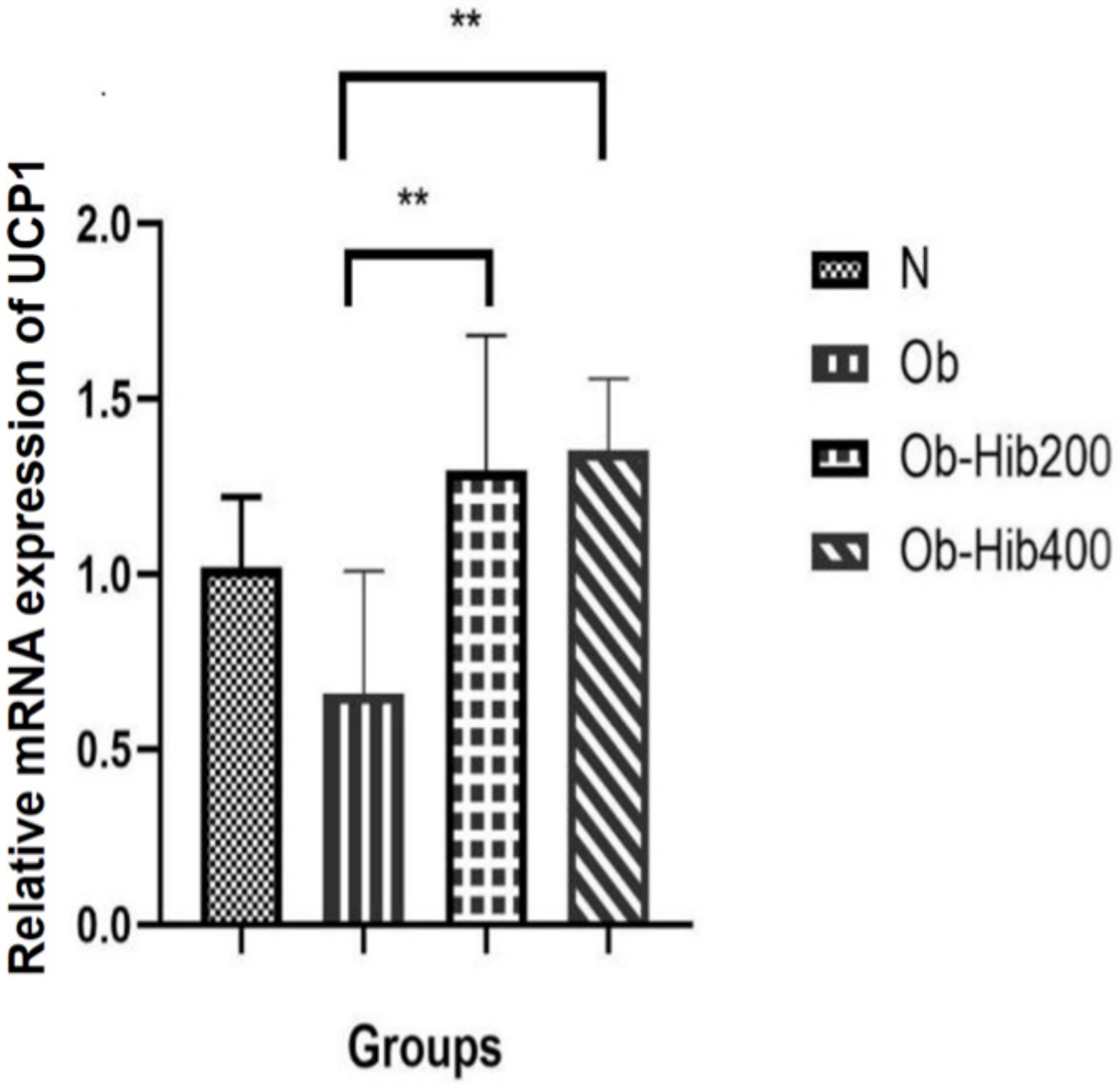

Figure 8

Average Ucp1 expression Data are depicted as mean ± SD. Significant differences are shown as *p<0.05, **p<0.01, ***p<0.001. N: Normal control group; Ob: DIO rats; Ob-Hib 200: DIO rats administered with HSE at a dose of 200 mg/kgBW; Ob-Hib 400: DIO rats administered with HSE at a dose of 400 mg/kgBW; SD: standard deviation, HSE: H. Sabdariffa.

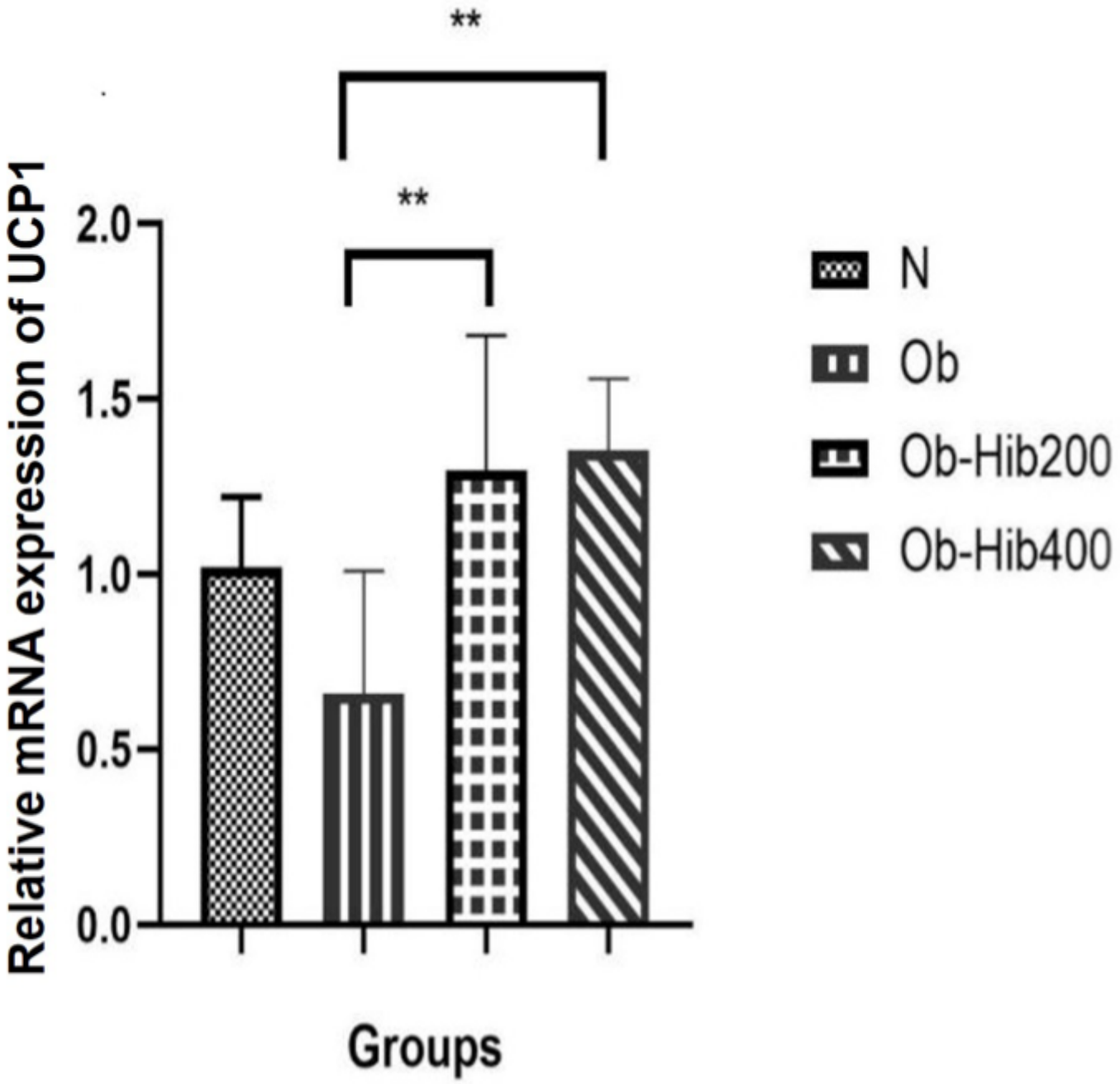

Figure 8

Average Ucp1 expression Data are depicted as mean ± SD. Significant differences are shown as *p<0.05, **p<0.01, ***p<0.001. N: Normal control group; Ob: DIO rats; Ob-Hib 200: DIO rats administered with HSE at a dose of 200 mg/kgBW; Ob-Hib 400: DIO rats administered with HSE at a dose of 400 mg/kgBW; SD: standard deviation, HSE: H. Sabdariffa.